Chapter 4
Piezoelectrically Active Acoustic Propagation

4.1 INTRODUCTION

Piezoelectricity, which means "pressing" electricity, is the link between electrical and mechanical phenomena. It is found experimentally that a polarization vector **P** (not to be confused with the polarizations of electromagnetic or acoustic waves!) is created if certain classes of crystals are subject to stress (or strain). Like the mechanical variables, **T** and **S**, where the presence of one automatically implies the other, in piezoelectric bodies a polarization is *coupled* to stress (or strain), and *vice versa*. The coupling matrix is somewhat simpler than that between stress and strain, where both variables are matrices because **P** is a vector. As in mechanical coupling, the number of independent variables in the piezoelectric matrices of a particular crystal depends on the symmetry class.

The presence of piezoelectricity modifies the propagation characteristics (phase velocities and polarizations) of the acoustic modes. We develop the Christoffel equation for piezoelectric classes, show the dependence of piezoelectricity on the crystal orientation $\hat{\mathbf{l}}$, and solve several important crystal orientations in detail. Finally, we add the piezoelectric correction to the computer program, which allows us to obtain the complete solution of acoustic propagation in all symmetry classes.

4.2 STATIC PIEZOELECTRICITY

Piezoelectricity involves the coupling between the mechanical properties (stress and strain) and the electrical properties of a crystal; the linkage of these two seemingly unrelated areas occurs through the polarization vector **P**.

All materials *polarize* to some degree. An electric field causes a physical separation between positive and negative charges, creating a *dipole* moment/volume **p**. The **P** polarization is defined as

$$\mathbf{P} = N\mathbf{p} \tag{4.1}$$

where N is the number of dipoles/volume. The units of **p** and **P** are $C \cdot m$ and C/m^2. Note that the polarization is a vector and, in general, is proportional to the electric field:

$$\mathbf{P} = \epsilon_0 \kappa \mathbf{E} \tag{4.2}$$

where **E** is the external electric field, $\epsilon_0 = 8.85 \times 10^{-12}$ F/m is the permittivity of free space and the electric susceptibility κ provides the connection between **P** and **E**. The susceptibility is a property of the material only and tells how easily a material polarizes when subjected to an **E** field. Both **E** and **P** are vectors, so κ must be a 3×3 matrix; for example,

$$P_i = \epsilon_0(\kappa_{i1}E_1 + \kappa_{i2}E_2 + \kappa_{i3}E_3) = \epsilon_0 \sum_1^3 \kappa_{ik}E_k$$

$$= \epsilon_0 \kappa_{ik}E_k, \qquad i = 1, 2, 3 \tag{4.3}$$

where, as usual, the double subscript implies a summation. Equation (4.3) expresses the important fact that the polarization is not necessarily in the same direction as **E**. This may occur, for example, if the charges are constrained at certain symmetry directions (which constrains the direction of **P**) while the external field is skewed to these directions.

We define the displacement vector **D** as

$$\mathbf{D} = \epsilon_0\mathbf{E} + \mathbf{P} = \epsilon_0\mathbf{E} + \epsilon_0\kappa\mathbf{E} \tag{4.4}$$

In double sum notation,

$$D_i = \epsilon_{ij}E_j \tag{4.5}$$

Comparing (4.4) and (4.5), we have

$$\epsilon_{ij} = \epsilon_0(1 + \kappa_{ij}) \tag{4.6}$$

For an isotropic medium, the ϵ matrix reduces to a scalar, and

$$\epsilon_{ij} = \epsilon_r\epsilon_0 \tag{4.7}$$

where ϵ_r is the relative dielectric constant and is a real positive number greater than 1. In free space,

$$\epsilon_r = 1 \quad \text{and} \quad \kappa = 0$$

In a piezoelectric medium, a polarization vector is created not only by an external electric field but also by a strain (or, equivalently, a stress) that deforms the crystal lattice and causes charge separation (i.e., a dipole moment per unit volume). The stress may be caused by an external body force, a nonuniform temperature distribution, or a dislocation in the crystal lattice. The resulting polarization is in addition to that caused by the application of an external electric field. We write

$$\mathbf{P} = \mathbf{d}:\mathbf{T} \tag{4.8}$$

Because **P** has units of C/m^2, the units of **d** are C/N. In this case, (4.5) is no longer valid; **D** has two components: one proportional to **E**, and one to **T**. Although all materials polarize on application of an **E** field, a stress does not always result in a polarization vector. The coupling of a polarization and stress depends on the symmetry class of the material. This principle is illustrated in Figure 4.1. In Figure 4.1(a), an external **E** field causes a polarization, but application of the symmetric forces does not. In Figure 4.1(b), the stress forces cause a distortion, which results in the left side becoming more positively charged and the right side more negatively charged. Although both crystals depicted in Figures 4.1(a) and 4.1(b) possess hexagonal symmetry, they belong to different subclasses. For the piezoelectric class, we rewrite (4.8) in double subscript notation:

$$P_k = \mathbf{d}T_{ij} \tag{4.9}$$

Following the rules for double subscript notation, we note that all repeated subscripts are "dummy" subscripts. The *matrix* **d** is called the piezoelectric strain matrix (for reasons which will be apparent later); it must possess two subscripts to sum with the stress matrix and a third to account for the kth component of **P** (recall that **c** required four subscripts to couple the stress and strain matrices). Equation 4.9 becomes

$$P_k = d_{kij}T_{ij} \tag{4.10}$$

where a double sum (over i and j) is implied. For example,

$$\begin{aligned} P_1 = {} & d_{111}T_{11} + d_{112}T_{12} + d_{113}T_{13} + d_{121}T_{21} + d_{122}T_{22} \\ & + d_{123}T_{23} + d_{131}T_{31} + d_{132}T_{32} + d_{133}T_{33} \end{aligned} \tag{4.11}$$

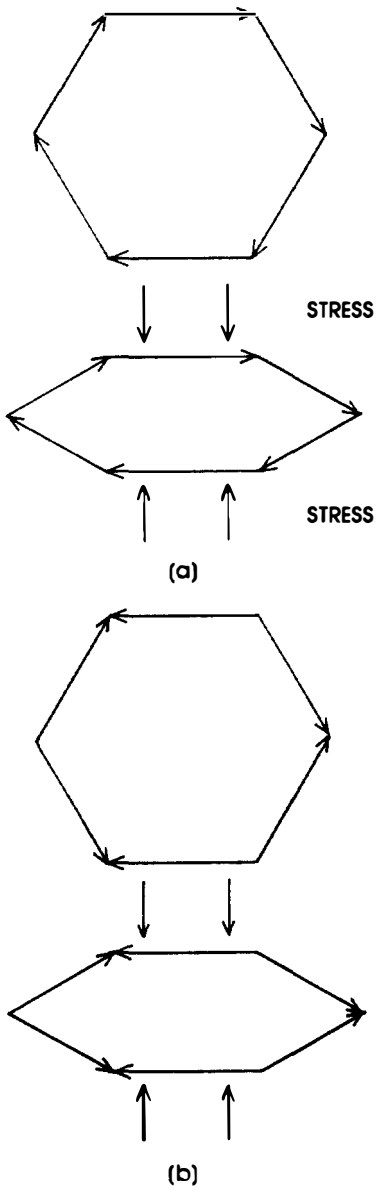

Figure 4.1 Coupling of a stress to an electric polarization. The arrows represent individual dipole moments. Even though both symmetry classes pictured are hexagonal, only in (b) does a stress couple to an electrical polarization.

There are nine terms (one for each stress component), and three polarization components, each with nine terms. Thus, the **d** matrix possesses a total of 27 terms. As we might expect, however, not all 27 are independent. Because $T_{ij} = T_{ji}$ (symmetry of the stress matrix), three of the terms in each polarization are not independent (9 out of 27). Thus, there are 18 independent components, and we can write

$$P_i = d_{iJ}T_J \qquad i = 1 \text{ to } 3, \quad \text{J} = 1 \text{ to } 6$$

The fact that a stress or strain produces an electrical response necessarily implies the inverse effect, namely, that the application of an electric field will result in a mechanical response. This is completely analogous to the relation of stress and strain; we say that the phenomena are *coupled*. Unlike the stress-strain coupling, however, there are three possible electrical variables (**E, P**, and **D**) and two mechanical variables (**S** and **T**). The inverse piezoelectric effect is defined through the relation:

$$S_J = d'_{Ji}E_i \qquad J = 1 \text{ to } 6, \quad i = 1 \text{ to } 3 \tag{4.12}$$

where d'_{Ji} is a 6×3 matrix called the *piezoelectric strain matrix*; it is the transpose of d_{iJ}. Using thermodynamics arguments, Nye [2] proves the relation between **d′** and **d**. In a nonrigorous proof based on a dimensional analysis, we assume that **d′** has the same units as **d**. Thus,

$$[\mathbf{d}'][\mathbf{E}] = (\text{C/N})(\text{V/m}) = (\text{C/N})(\text{N} \cdot \text{m/C} \cdot \text{m}) \tag{4.13}$$

Because the strain is also dimensionless, our assertion that **d** and **d′** have the same dimensions is valid. We will use the two matrices interchangeably and drop the prime (from (4.12) it is obvious why **d** is called the piezoelectric strain matrix). As usual, the existence of the double subscript on the right side implies a summation over i, so each of the six strain components contains three terms. To summarize our results, we write

$$P_i = \kappa_{ij}\epsilon_0 E_j + d_{iJ}T_J \tag{4.14}$$

$$S_J = d_{Jk}E_k + s_{JK}T_K \tag{4.15}$$

To limit the electrical variables to **E** and **D**, we substitute (4.4) in (4.14):

$$D_i = \epsilon_{ij}^{\text{T}}E_j + d_{iJ}T_J \tag{4.16}$$

$$S_J = d_{Jk}E_k + s^{\mathbf{E}}_{JK}T_K \tag{4.17}$$

The first term in (4.16) and the second term in (4.17) represent the "normal" piezoelectrically uncoupled equations, which are always valid. The other terms (involving the **d** matrix) are valid only for certain symmetry classes. The superscripts **T** and **E** denote that the permittivity and compliance must be measured under conditions of constant stress and electric field. For example, suppose that we apply an **E** field that produces both a displacement **D** and a strain **S**; the strain, in turn, is coupled to a stress that *changes* the relation between **D** and **E**. To eliminate this multiple coupling, we require that the permittivity of a piezoelectric material be measured at constant, usually zero, stress. Practically, this requirement means that the body must be allowed to expand or contract without constraints.

Equations (4.16) and (4.17) can easily be modified so that the strain is the independent variable; we multiply (4.17) by the stiffness matrix:

$$c^{\mathbf{E}}_{KJ}S^{\mathbf{E}}_J = c^{\mathbf{E}}_{KJ}d_{Jk}E_k + c_{KJ}s_{JK}T_K \tag{4.18}$$

The superscript **E** reminds us that when we measure the mechanical constants we must ground the crystal to prevent charge buildup, which could significantly alter (4.18). We use

$$\mathbf{c{:}s} = \mathbf{I} \text{ (the identity matrix)}$$

and define

$$e_{Kk} = (c^{\mathbf{E}}_{KJ})d_{Jk} \tag{4.19}$$

(note the double summation over the dummy variable J). From (4.19), the units of the e components are C/m^2. Equation (4.17) is written as

$$T_K = -e_{Kk}E_k + c^{\mathbf{E}}_{KJ}S_J \tag{4.20}$$

To transform (4.17) so that the strain is the independent variable, we substitute (4.20) for T_K:

$$D_i = \epsilon^{\mathbf{T}}_{ik}E_k + d_{iK}(-e_{Kk}E_k + c^{\mathbf{E}}_{KJ}S_J) \tag{4.21}$$

Expanding gives

$$D_i = (\epsilon^{\mathbf{T}}_{ik} - d_{iK}e_{Kk})E_k + d_{iK}c^{\mathbf{E}}_{KJ}S_J$$

Finally,

$$D_i = \epsilon_{ik}^{S} E_k + e_{iJ} S_J \tag{4.22}$$

where

$$\epsilon_{ik}^{S} = \epsilon_{ik}^{T} - d_{iK} e_{Kk} = \epsilon_{ik}^{T} - d_{iK} c_{KJ}^{E} d_{Jk} \tag{4.23}$$

is the permittivity at constant *strain*, and e_{iJ} is a 3×6 matrix, the transpose of e_{Ji}. The matrix **e** is called the *piezoelectric stress matrix*; it has the same symmetry as the piezoelectric strain matrix **d**.

Rewriting (4.20) and (4.22), we obtain

$$\mathbf{T} = -\mathbf{e}:\mathbf{E} + \mathbf{c}^{E}:\mathbf{S} \tag{4.24}$$

$$\mathbf{D} = \boldsymbol{\epsilon}^{S}:\mathbf{E} + \mathbf{e}:\mathbf{S} \tag{4.25}$$

The form of (4.16) and (4.17), in which **T** is the independent variable, is most useful in statics problems (in which forces are applied); the form of (4.24) and (4.25), in which **S** is the independent variable, is useful in acoustic wave calculations because the strain is related to polarization by (1.86). We will be using $\boldsymbol{\epsilon}^{S}$ for the permittivity of piezoelectric materials; for nonpiezoelectric materials, $\mathbf{d} = \mathbf{e} = 0$ and $\boldsymbol{\epsilon}^{T} = \boldsymbol{\epsilon}^{S}$, whereas for piezoelectric materials they may be quite different. Indeed, the difference is a measure of the piezoelectricity of the crystal. Because (4.23) is a matrix equation, it is clear that the difference depends on the particular directional properties of the crystal cut. Additionally, because the measurement of $\boldsymbol{\epsilon}^{S}$ requires that the crystal be rigidly clamped to prevent any motion, including shear, this measurement is very difficult to carry out. Thus, to find $\boldsymbol{\epsilon}^{S}$, we measure $\boldsymbol{\epsilon}^{T}$ and use (4.23).

4.3 SYMMETRY OF THE PIEZOELECTRIC MATRICES

We assume that

1. **d** and **e** have the same symmetry (like the stiffness and and compliance matrices, the forms are identical except for factors of 2);
2. $\mathbf{e}_{iK} = \tilde{\mathbf{e}}_{Ki}$.

The piezoelectric matrix contains only null components if the symmetry class has a center of symmetry. This operator reverses the signs of all components and is represented by the matrix:

$$\delta = \begin{bmatrix} -1 & 0 & 0 \\ 0 & -1 & 0 \\ 0 & 0 & -1 \end{bmatrix}$$

Application of δ causes

$$x \rightarrow -x \quad y \rightarrow -y \quad z \rightarrow -z$$

or

$$1 \rightarrow -1 \quad 2 \rightarrow -2 \quad 3 \rightarrow -3$$

Now consider the **d** matrix in the most general symmetry:

$$\mathbf{d} = \begin{bmatrix} d_{11} & d_{12} & d_{13} & d_{14} & d_{15} & d_{16} \\ d_{21} & d_{22} & d_{23} & d_{24} & d_{25} & d_{26} \\ d_{31} & d_{32} & d_{33} & d_{34} & d_{35} & d_{36} \end{bmatrix}$$

Reversing the signs of all the coordinates changes the signs of the components. For example, consider the first term:

$$d_{11} = d_{1(11)}$$

Applying the δ operator gives

$$111 \rightarrow (-1)(-1)(-1) \rightarrow \mathrm{d}_{111} \rightarrow -d'_{111}$$

but because we assume that a symmetry operation (in this case δ) leaves all physical properties unchanged (Neumann's principle), we require that

$$d_{11} = -d'_{1(11)} = -d'_{11}$$

or

$$d_{11} = 0$$

Similar conclusions apply to all components of **d**, and thus **d** is the null matrix if δ is a valid symmetry operation of a particular class. An example of such a symmetry is the nonpiezoelectric hexagonal class in Figure 4.1(a). This symmetry condition is also true for *all* physical properties that can be represented by mathematical entities containing an *odd*

number of subscripts. An important example is pyroelectricity, which couples a change in polarization (an electrical property and a vector) to a change in temperature (a scalar); we write

$$\mathbf{P} = \mathbf{p}\,\Delta T \tag{4.26}$$

where $\mathbf{P}$ is the contribution to the polarization due to a temperature change ΔT, and $\mathbf{p}$ is the pyroelectric matrix. Because temperature is a scalar, the pyroelectric matrix has the same dimensions as the polarization vector, namely, 3×1 (or 1×3). In this case, the center of symmetry operator changes each component singly, as compared with the piezoelectric matrix, where each component was changed as a triplet. The result is identical, namely, that all elements are zero. Only 10 classes (out of 32) exhibit pyroelectricity, and all nonpiezoelectric materials are also not pyroelectric. The 10 piezoelectric classes are distributed among all the symmetry systems except the isotropic. Each system is thus composed of some classes that are piezoelectric and some that are not (except the triclinic).

Next we consider a symmetry operation that does not result in all zero elements: The operation is a rotation of 180° around the z-axis and is represented by the matrix:

$$\begin{bmatrix} -1 & 0 & 0 \\ 0 & -1 & 0 \\ 0 & 0 & 1 \end{bmatrix} \quad \begin{matrix} x \to -x & y \to -y & z \to z \\ 1 \to -1 & 2 \to -2 & 3 \to 3 \end{matrix}$$

Operating on $\mathbf{d}$ component by component, we find

$$\begin{aligned} d_{11} &= d_{111} \to -d'_{111} \quad \text{or} \quad d_{11} = 0 \\ d_{22} &= d_{222} \to -d'_{222} \quad \text{or} \quad d_{22} = 0 \\ d_{33} &= d_{333} \to d'_{333} \qquad \text{independent component} \\ d_{14} &= d_{123} \to d'_{123} \qquad \text{independent component} \\ d_{15} &= d_{113} \to d'_{15} \qquad \text{independent component} \end{aligned}$$

The piezoelectric stress matrix transforms under this operation to:

$$\mathbf{d} = \begin{bmatrix} 0 & 0 & 0 & d_{14} & d_{15} & 0 \\ 0 & 0 & 0 & d_{24} & d_{25} & 0 \\ d_{31} & d_{32} & d_{33} & 0 & 0 & d_{36} \end{bmatrix} \tag{4.27}$$

To find the exact form of the piezoelectric matrix for a particular class, we must apply the relevant operations; a class containing additional

symmetry operations could have other zero components in (4.27), but it could not have a nonzero component in a place where (4.27) shows a zero. Consider, for example, a 180° rotation about the x-axis:

$$\mathbf{A} = \begin{bmatrix} 1 & 0 & 0 \\ 0 & -1 & 0 \\ 0 & 0 & -1 \end{bmatrix} \begin{array}{llll} x \rightarrow x & 1 \rightarrow 1 & 4 \rightarrow 4 \\ y \rightarrow -y & 2 \rightarrow -2 & 5 \rightarrow -5 \\ z \rightarrow -z & 3 \rightarrow -3 & 6 \rightarrow -6 \end{array}$$

Applying **A** to (4.27), we immediately obtain

$$d_{15} = d_{33} = d_{24} = d_{31} = d_{32} = 0$$

The **d** matrix becomes

$$\mathbf{d} = \begin{bmatrix} 0 & 0 & 0 & d_{14} & 0 & 0 \\ 0 & 0 & 0 & 0 & d_{25} & 0 \\ 0 & 0 & 0 & 0 & 0 & d_{36} \end{bmatrix} \tag{4.28}$$

Finally, for cubic symmetry, we can use the change of axis matrix (2.73):

$$\mathbf{A} = \begin{bmatrix} 0 & 1 & 0 \\ 0 & 0 & 1 \\ 1 & 0 & 0 \end{bmatrix} \begin{array}{llll} x \rightarrow y & 1 \rightarrow 2 & 4 \rightarrow 5 \\ y \rightarrow z & 2 \rightarrow 3 & 5 \rightarrow 6 \\ z \rightarrow x & 3 \rightarrow 1 & 6 \rightarrow 4 \end{array}$$

Applying this symmetry operation to (4.28), we find that

$$d_{14} = d_{25} = d_{36}$$

The piezoelectric strain matrix for cubic crystals contains only one independent constant.

The procedure for tetragonal and orthorhombic crystals is carried out similarly. The tetragonal class $\bar{4}2m$, for example, does not possess the change of axis symmetry operation (only the x- and y-axes are identical); it is not surprising that **d** for this class is

$$\mathbf{d} = \begin{bmatrix} 0 & 0 & 0 & d_{14} & 0 & 0 \\ 0 & 0 & 0 & 0 & d_{14} & 0 \\ 0 & 0 & 0 & 0 & 0 & d_{36} \end{bmatrix}$$

For trigonal and hexagonal symmetries, the procedure is somewhat more complex. The symmetry elements involve 60° and 120° rotations about the z-axis:

$$60° \rightarrow \begin{bmatrix} 1/2 & \sqrt{3}/2 & 0 \\ -\sqrt{3}/2 & 1/2 & 0 \\ 0 & 0 & 1 \end{bmatrix}, \qquad 120° \rightarrow \begin{bmatrix} -1/2 & \sqrt{3}/2 & 0 \\ -\sqrt{3}/2 & -1/2 & 0 \\ 0 & 0 & 1 \end{bmatrix}$$

Applying these operations to the general piezoelectric strain matrix (4.25) results in sets of coupled simultaneous equations, because the axes do not transform as simply as in 90° rotations. The procedure of applying 60° and 120° rotations can also be used in principle to develop the form of the stiffness matrix for the trigonal and hexagonal classes. However, for the more complex (6 × 6) form of **c**, it is usually easier to employ alternative methods. With this technique, the form of the **d** matrix for the class $3m$ is

$$\mathbf{d} = \begin{bmatrix} 0 & 0 & 0 & 0 & d_{15} & -2d_{22} \\ -d_{22} & d_{22} & 0 & d_{15} & 0 & 0 \\ d_{31} & d_{31} & d_{33} & 0 & 0 & 0 \end{bmatrix} \tag{4.29}$$

For lithium niobate, we have

$$d_{15} = 68 \ (\times 10^{-12} \text{ C/N})$$

$$d_{22} = 21$$

$$d_{31} = -1$$

$$d_{33} = 6$$

If a force is applied by pressing along one of the major axes, a longitudinal stress will be momentarily created in the direction of the force. This in turn will cause a voltage to be developed in the crystal, which can be measured with a very high impedance voltmeter. A high impedance is required because the electrical impedance of the crystal is usually extremely large and is very easily "loaded." A typical experimental configuration is shown in Figure 4.2.

For lithium niobate, the presence of a longitudinal directed stress T_1 does not result in a voltage measured parallel to the x-axis because $d_{11} = 0$. However, for the same stress, a voltage will be developed in both the y and z planes due to the presence of d_{22} and d_{31}. Furthermore, for a constant crystal thickness and external force, the voltage developed across electrodes in the y sides will be significantly larger than that across the z sides because $d_{22} \gg d_{31}$. For T_3, there will be a voltage developed across electrodes attached to the z sides of the crystal due to the presence of d_{33}.

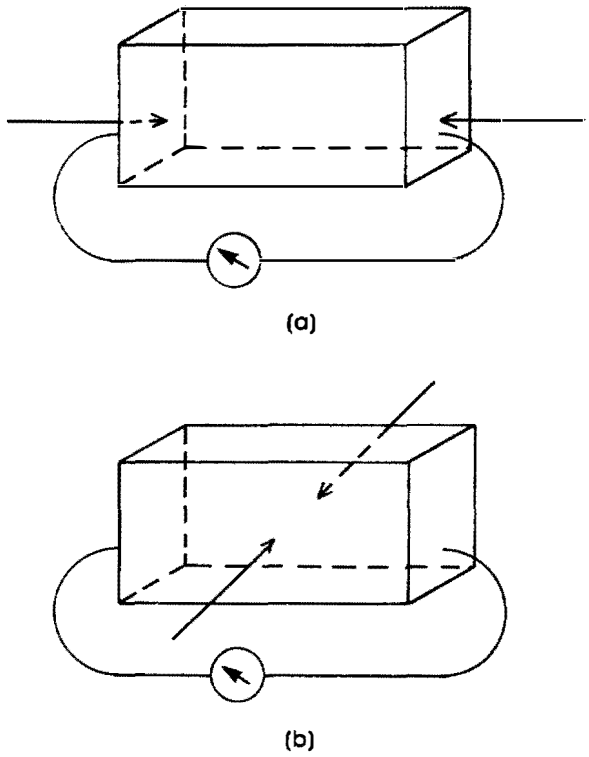

Figure 4.2 Experimental configuration for qualitative determination of piezoelectric constants: (a) determination of d_{ii}; (b) determination of d_{ij}.

Typical strip chart recordings for various experimental configurations using lithium niobate are shown in Figure 4.3. This is a practical technique to determine the axes of a crystal of unknown orientation.

4.5 CHRISTOFFEL EQUATION FOR PIEZOELECTRIC CRYSTALS

Recall the comparison of the electrical and acoustic equations from Table 4.1. As we have seen, the property of piezoelectricity couples the two sets of equations. This is reflected in the constitutive relations.

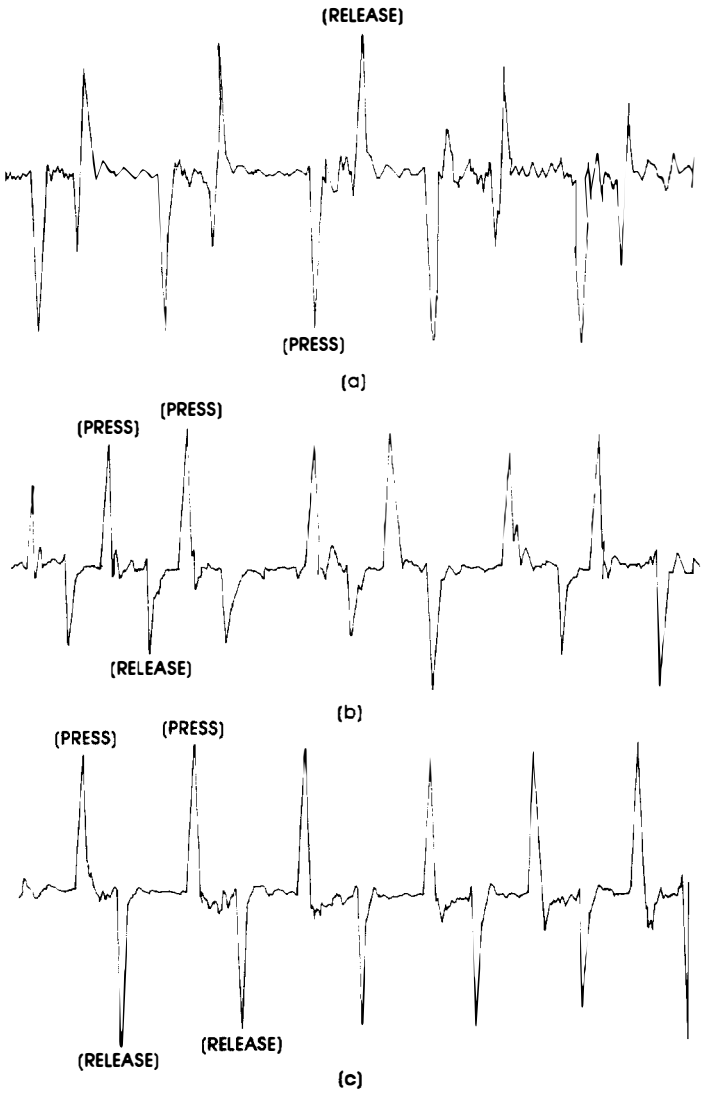

Figure 4.3 Strip chart recordings of press test measurement (Figure 4.2) for lithium niobate: (a) press y measure along y determines d_{22}; (b) reversing the electrodes reverses the sign of the voltage; (c) press x measure along y determines $d_{21} = -d_{22}$.

Table 4.1

Electrical	*Acoustic*
Faraday's law	Newton's law
$\nabla \times \mathbf{E} = -\frac{\partial \mathbf{B}}{\partial t}$	$\nabla \cdot \mathbf{T} = \rho \frac{\partial \mathbf{v}}{\partial t}$
Ampere's law	Definition of strain
$\nabla \times \mathbf{H} = \frac{\partial \mathbf{D}}{\partial t} + \mathbf{J}$	$\nabla_S \mathbf{v} = \frac{\partial \mathbf{S}}{\partial t}$
$\mathbf{B} = \mu \mathbf{H}$	$\mathbf{v} = \frac{\partial \mathbf{u}}{\partial t}$
Uncoupled (nonpiezoelectric)	
$\mathbf{D} = \epsilon \cdot \mathbf{E}$	$\mathbf{T} = \mathbf{c}:\mathbf{S}$
Coupled (piezoelectric)	
$\mathbf{D} = \epsilon^{\mathbf{S}} \cdot \mathbf{E} + \mathbf{e}:\mathbf{S}$ (4.25)	$\mathbf{T} = -\mathbf{e}:\mathbf{E} + \mathbf{c}^{\mathbf{E}}:\mathbf{S}$ (4.24)

The fundamental physical laws (Faraday's and Ampere's laws in the electrical case and the strain equation and Newton's law in the acoustic case) are not altered by piezoelectricity. We multiply the strain equation by $\mathbf{c}^{\mathbf{E}}$:

$$\mathbf{c}^{\mathbf{E}}:\nabla_S \mathbf{v} = \mathbf{c}^{\mathbf{E}}:\frac{\partial \mathbf{S}}{\partial t} \tag{4.30}$$

Next, we differentiate (4.24) with respect to t:

$$\mathbf{c}^{\mathbf{E}}:\frac{\partial \mathbf{S}}{\partial t} = \frac{\partial \mathbf{T}}{\partial t} + \mathbf{e}:\frac{\partial \mathbf{E}}{\partial t} \tag{4.31}$$

Rearranging and using (4.30), we get

$$\frac{\partial \mathbf{T}}{\partial t} = \mathbf{c}^{\mathbf{E}}:\frac{\partial \mathbf{S}}{\partial t} - \mathbf{e}:\frac{\partial \mathbf{E}}{\partial t} = \mathbf{c}^{\mathbf{E}}:\nabla_S \mathbf{v} - \mathbf{e}:\frac{\partial \mathbf{E}}{\partial t} \tag{4.32}$$

Differentiating Newton's law gives

$$\nabla \cdot \frac{\partial \mathbf{T}}{\partial t} = \rho \frac{\partial^2 \mathbf{v}}{\partial t^2} \tag{4.33}$$

Substituting (4.32) into (4.33), we have

$$\nabla \cdot \mathbf{c}^{\mathbf{E}}:\nabla_S\mathbf{v} - \nabla \cdot \mathbf{e}:\frac{\partial \mathbf{E}}{\partial t} = \rho \frac{\partial^2 \mathbf{v}}{\partial t^2} \tag{4.34}$$

Equation (4.34) is the Christoffel equation with an electrical perturbation.

We next consider the electromagnetic wave equation in three dimensions (letting $\mathbf{J} = 0$):

$$-\nabla \times \nabla \times \mathbf{E} = \mu_0 \frac{\partial^2 \mathbf{D}}{\partial t^2} \tag{4.35}$$

Using (4.25), we get

$$-\nabla \times \nabla \times \mathbf{E} = \mu_0 \boldsymbol{\epsilon}^{\mathbf{S}}:\frac{\partial^2 \mathbf{E}}{\partial t^2} + \mu_0 \mathbf{e}:\frac{\partial^2 \mathbf{S}}{\partial t^2} \tag{4.36}$$

Eliminating the strain term by substituting (2.37), we thus obtain

$$-\nabla \times \nabla \times \mathbf{E} = \mu_0 \boldsymbol{\epsilon}^{\mathbf{S}}:\frac{\partial^2 \mathbf{E}}{\partial t^2} + \mu_0 \mathbf{e}:\nabla_S\left(\frac{\partial \mathbf{v}}{\partial t}\right) \tag{4.37}$$

Equation (4.37) is the electromagnetic wave equation with an acoustic perturbation term.

Equations (4.34) and (4.37) are the equations that we seek; they couple the electric field $\mathbf{E}$ to the acoustic field $\mathbf{v}$; in the absence of piezoelectricity $\mathbf{e} \rightarrow 0$, they reduce to the "regular" uncoupled wave equations for the acoustic and electric fields. In (4.34),

$$\nabla \cdot \mathbf{c}:\nabla_S\mathbf{v} \rightarrow \nabla_{iK} c_{kL} \nabla_{Lj}(v_j)$$

where ∇_{iK} and ∇_{Lj} are defined by (1.85) and (1.91). For plane waves,

$$\nabla_{iK} c_{KL} \nabla_{Lj} \rightarrow \Gamma_{ij} \quad \text{(the Christoffel matrix)}$$

We next evaluate the coupling terms in (4.34) and (4.37). The electrical coupling term in (4.34) is

$$\nabla \cdot \mathbf{e}:\frac{\partial \mathbf{E}}{\partial t}$$

Because $\partial \mathbf{E}/\partial t$ is a 3×1 matrix and $\mathbf{e}$ is a 6×3 matrix, their product is a 6×1 matrix. Recall from (1.91) that $\nabla \cdot \rightarrow \nabla_{iJ}$ converts a 6×1 matrix into a 3×1 matrix. We write

$$\nabla \cdot \mathbf{e}:\frac{\partial \mathbf{E}}{\partial t} \rightarrow \nabla_{iJ} e_{Jk} \frac{\partial E_k}{\partial t} \underset{\text{plane waves}}{\rightarrow} -jkl_{iJ} e_{Jk} \frac{\partial E_k}{\partial t} \tag{4.38}$$

The perturbation term must be a vector to be consistent with the other terms in (4.34). The acoustic perturbation in the electromagnetic wave equation is

$$\mu_0 \mathbf{e}:\nabla_S \frac{\partial \mathbf{v}}{\partial t}$$

This term is easily seen to possess the form of a 3×1 matrix (i.e., a vector) as it must. Analogously to (4.38);

$$\mu_0 \mathbf{e}:\nabla_S \frac{\partial \mathbf{v}}{\partial_t} \rightarrow \mu_0 e_{iI} \nabla_{Ij} v_j \underset{\text{plane waves}}{\rightarrow} \mu_0 e_{iI}(-jkl_{Ij}) v_j \tag{4.39}$$

Returning to (4.34) and (4.37), we assume that the presence of the acoustic wave does not cause electromagnetic radiation in the crystal; that is, there is no coupling between **E** (created by the acoustic wave) and **H**, and thus there is no electromagnetic energy carried due to the acoustic wave. This assumption is called the *quasistatic approximation*; if it were not valid, crystal cuts that were piezoelectrically active would display an extra acoustic loss mechanism through coupling to an electromagnetic radiation. No such loss mechanism has been observed, even in strongly piezoelectric materials operating at frequencies as high as 10 GHz. Indeed, some of the lowest acoustic attenuations have been measured in piezoelectrically active crystal cuts.

The assumption that there is no coupling to an electromagnetic wave with an acoustic wave, and thus no acoustically generated magnetic field, implies that

$$\nabla \times \mathbf{E} = 0 \tag{4.40}$$

From (4.40), we can write the electric field as the gradient of a scalar potential:

$$\mathbf{E} = -\nabla \phi \tag{4.41}$$

The implication of (4.40) is that the electric field continuously being generated by the strain wave propagates at the *acoustic* velocity. Furthermore, from (4.41), because the spatial variation of the electric potential varies only in the direction of the acoustic wave (we assume a plane wave), the

electric field is in the direction of $\hat{\mathbf{l}}$; i.e., it is a *longitudinal* field (for example, if the acoustic wave is z-propagating, then $\mathbf{E} = E(\mathbf{r},t)\hat{\mathbf{k}}$). This property will take on increased significance later. The left side of (4.36) is now zero. Substituting (4.41) into (4.37) and taking the divergence of (4.37), we obtain

$$\nabla \cdot \mathbf{c}{:}\nabla_S \mathbf{v} - \rho \frac{\partial^2 \mathbf{v}}{\partial t^2} = -\nabla \cdot \mathbf{e}{:}\frac{\partial \nabla \phi}{\partial t} \tag{4.34}$$

and

$$0 = -\mu_0 \nabla \cdot \boldsymbol{\epsilon}^{\mathbf{S}}{:}\frac{\partial^2 \nabla \phi}{\partial t^2} + \mu_0 \nabla \cdot \left(\mathbf{e}{:}\,\nabla_S \frac{\partial \mathbf{v}}{\partial t}\right) \tag{4.42}$$

Next, we convert to the plane wave formalism:

$$-k^2(l_{iK}c_{KL}l_{Lj})v_j + \rho\omega^2 v_i = j\omega k^2 (l_{iK}e_{Kj}l_j)\phi \tag{4.43}$$

because $\nabla\phi \rightarrow (l_j\phi)\,(-jk)$, and

$$0 = \omega^2 k^2 (l_i \epsilon_{ij}^{\mathbf{S}} l_j)\phi - j\omega k^2 (l_i e_{iL} l_{Lj}) v_j \tag{4.44}$$

Equations (4.43) and (4.44) are a set of two equations in two unknowns, one acoustic ($\mathbf{v}$) and one electric (ϕ). Solving (4.44) for ϕ gives

$$\phi = \frac{1}{j\omega}\left(\frac{(l_i e_{iL} l_{Lj})v_j}{l_i \epsilon_{ij}^{\mathbf{S}} l_j}\right) \tag{4.45}$$

Substituting (4.45) into (4.43) gives the result we want:

$$k^2\left(l_{iK}\left(c_{KL}^{\mathbf{E}} + \frac{(e_{Kj}l_j)(l_i e_{iL})}{l_i \epsilon_{ij}^{\mathbf{S}} l_j}\right) l_{Lj}\right) v_j = \rho\omega^2 v_i \tag{4.46}$$

Compared with the nonpiezoelectric Christoffel equation (2.48):

$$k^2(l_{iK}c_{KL}l_{Lj})v_j = \rho\omega^2 v_i$$

we see that the form is identical, but that extra terms, dependent on the piezoelectric and permittivity matrices, have been added to the stiffness matrix. We say that the components of the stiffness matrix have been piezoelectrically *stiffened*. The products of the terms $[e_{Kj}l_j]$ and $[l_i e_{iL}]$ are

components of a 6 × 6 matrix, because the first terms are components of a 6 × 3 matrix and the second are components of a 3 × 6 matrix, and the term $l_i \epsilon_{ij}^{\mathbf{S}} l_j$ is a scalar. For a given propagation direction $\hat{\mathbf{l}}$, the form of the stiffness components is

$$c' = c^{\mathbf{E}} + \frac{e^2}{\epsilon^{\mathbf{S}}} \tag{4.47}$$

The phase velocity is determined by c' rather than by c, and is

$$v_a = \frac{\omega}{k} = \left(\frac{c^{\mathbf{E}}}{\rho}\left(1 + \frac{e^2}{\epsilon^{\mathbf{S}} c^{\mathbf{E}}}\right)\right)^{1/2} \tag{4.48}$$

In addition to the fact that the acoustically generated electric field is longitudinal and propagates at the acoustic phase velocity, there is another important property of the electric fields associated with a piezoelectrically active acoustic wave. Consider (4.24) and (4.25), in which the displacement vector and stress vary only in the z direction (such behavior is characteristic of a plane acoustic wave propagating in z):

$$\mathbf{D} = \mathbf{e}:\mathbf{S} + \epsilon^{\mathbf{S}}:\mathbf{E} = e\frac{\partial u}{\partial z} + \epsilon^{\mathbf{S}} E \tag{4.49}$$

$$\mathbf{T} = \mathbf{c}^{\mathbf{E}}:\mathbf{S} - \mathbf{e}:\mathbf{E} = c^{\mathbf{E}}\frac{\partial u}{\partial z} - eE \tag{4.50}$$

Similarly, Newton's law becomes (from (1.6)):

$$\frac{\partial T}{\partial z} = \rho\frac{\partial S}{\partial t} = \rho\frac{\partial^2 u}{\partial t^2}$$

Combining (4.49) and (4.50), we get

$$D = e\frac{\partial u}{\partial z} + \epsilon^{\mathbf{S}}\left(-\frac{T}{e} + \frac{c^{\mathbf{E}}}{e}\frac{\partial u}{\partial z}\right) \tag{4.51}$$

For plane wave propagation, u varies sinusoidally:

$$u \propto e^{j(\omega t - kz)} \tag{4.52}$$

Using (4.51) and (1.12), we write the displacement vector as

$$D = \left(e(-jk) + \frac{\epsilon^S \rho\omega^2}{-jke} + \frac{\epsilon^S c^E}{e}(-jk)\right)u \tag{4.53}$$

Finally, substituting (4.48) into (4.53), we find that $D = 0$! In the piezoelectric medium, there is a longitudinal electric field without a proportional displacement vector. In view of (4.25), it probably should not come as a complete surprise that **D** is not proportional to **E**, as in a normal "dead" dielectric. The consequence of a vanishing D_z is that it is impossible to extract electrical energy from the piezoelectric medium (because there is no displacement current). Energy conversion is accomplished by using resonating structures, which we will study in Chapters 5 and 6.

4.5 HEXAGONAL AND TRIGONAL SYMMETRIES

The hexagonal and trigonal classes are closely associated with piezoelectricity. Included in these symmetries are the important crystals zinc oxide (ZnO) and cadmium sulfide (CdS), which are hexagonal, and lithium niobate ($LiNbO_3$), lithium tantalate ($LiTaO_3$), and quartz (SiO_2), which are trigonal. The form of the stiffness matrix cannot be determined by simple application of Neumann's principle because some of the symmetry elements are 60° and 120° rotations about the z-axis.

The form of **c** for the hexagonal classes is

$$\mathbf{c} = \begin{bmatrix} c_{11} & c_{12} & c_{13} & 0 & 0 & 0 \\ c_{12} & c_{11} & c_{13} & 0 & 0 & 0 \\ c_{13} & c_{13} & c_{33} & 0 & 0 & 0 \\ 0 & 0 & 0 & c_{44} & 0 & 0 \\ 0 & 0 & 0 & 0 & c_{44} & 0 \\ 0 & 0 & 0 & 0 & 0 & c_{66} \end{bmatrix}, \quad c_{66} = \frac{c_{11} - c_{12}}{2} \tag{4.54}$$

Equation (4.54) appears to be tetragonal, with the important difference that there is an "isotropy" condition on c_{66}. In the xy plane, the Christoffel matrix is (following the rules of (2.49) and (2.51)

$$\Gamma = \begin{bmatrix} c_{11}l_x^2 + c_{66}l_y^2 & (c_{12} + c_{66})l_x l_y & 0 \\ (c_{12} + c_{66})l_x l_y & c_{66}l_x^2 + c_{11}l_y^2 & 0 \\ 0 & 0 & c_{44}l_x^2 + c_{44}l_y^2 \end{bmatrix}, \quad l_x^2 + l_y^2 = 1 \tag{4.55}$$

As in tetragonal symmetry, there is a pure z-polarized shear wave with direction-independent velocity (slowness curve is a circle). Not so obvious

is the fact that the other two modes are also pure with direction-independent velocities. We can prove this by following the procedure outlined in (2.57) and (2.58). The slowness curves consist of three concentric circles, and the power flow angle for all modes is zero. As expected, in the xz and yz planes the slowness curves resemble those of the tetragonal symmetry, because the isotropy condition does not apply (recall that 6 represents xy in double subscript notation).

As an example of the hexagonal system, we solve the important case of piezoelectricity for a z-propagating pure longitudinal mode in ZnO. This crystal belongs to the class 6*mm* and has a piezoelectric stress matrix of the form,

$$\mathbf{e} = \begin{bmatrix} 0 & 0 & 0 & 0 & e_{15} & 0 \\ 0 & 0 & 0 & e_{15} & 0 & 0 \\ e_{31} & e_{31} & e_{33} & 0 & 0 & 0 \end{bmatrix}$$

where $e_{15} = -.48$, $e_{31} = -.57$, and $e_{33} = 1.32$. From (4.46), for the longitudinal z-propagating mode, $K = L = 3$, and because the mode is pure longitudinal, $v_j = v_3$. The piezoelectric correction terms become

$$e_{Kj}l_j = e_{33} = l_i e_{iL}$$

The stiffened stiffness constant is

$$c'_{33} = c_{33} + \frac{e_{33}^2}{\epsilon_r}$$

This is an important configuration, not only because ZnO is relatively easy to deposit oriented along the z-axis but also because the piezoelectric constant e_{33} is quite large.

The form of the stiffness matrix for the trigonal symmetry is

$$\mathbf{c} = \begin{bmatrix} c_{11} & c_{12} & c_{13} & c_{14} & 0 & 0 \\ c_{12} & c_{11} & c_{13} & -c_{14} & 0 & 0 \\ c_{13} & c_{13} & c_{33} & 0 & 0 & 0 \\ c_{14} & -c_{14} & 0 & c_{44} & 0 & 0 \\ 0 & 0 & 0 & 0 & c_{44} & c_{14} \\ 0 & 0 & 0 & 0 & c_{14} & c_{66} \end{bmatrix}, \quad c_{66} = \frac{c_{11} - c_{12}}{2} \tag{4.56}$$

We note that there is an isotropy condition for c_{66}, as in hexagonal symmetry. The symmetry is characterized by the terms c_{14}, c_{24}, and c_{56}, which

are present in all trigonal classes and result in interesting new propagation properties. The c_{14} and $-c_{14}$ terms in the first and second rows represent coupling between shear strain and longitudinal stress (the same terms in row 4 represent coupling between longitudinal strain and shear stress), and the $c_{56} = c_{14}$ term represents coupling between shear xz strain and shear xy stress.

An important result of the form of (4.56) is that in the xy and xz planes all modes are quasimodes. Only in the yz plane is there a pure (x-polarized) shear mode. We can derive this result by writing the Christoffel matrix explicitly, following the rules of (2.51). In the yz plane, the Christoffel matrix is

$$\Gamma = \begin{bmatrix} c_{66}l_y^2 + c_{44}l_z^2 + 2c_{14}l_yl_z & 0 & 0 \\ 0 & c_{11}l_y^2 + c_{44}l_z^2 - 2c_{14}l_yl_z & (c_{13} + c_{44})l_yl_z - c_{14}l_y^2 \\ 0 & (c_{14} + c_{44})l_yl_z - c_{14}l_y^2 & c_{44}l_y^2 + c_{33}l_z^2 \end{bmatrix} \tag{4.57}$$

The pure shear (x-polarized) mode has stiffness constant:

$$c = c_{66}l_y^2 + c_{44}l_z^2 + 2c_{14}l_yl_z \tag{4.58}$$

The right side of (4.58) has the form of a rotated ellipse, so the power flow angle will be zero only for two discrete angles. Note that if $c_{14} \rightarrow 0$, then the form of (4.58) is identical to the pure (x-polarized) shear mode in the yz plane for tetragonal symmetry (which is an unrotated ellipse). The forms of the quasilongitudinal and quasishear modes are quite complex and are best handled by computer solution.

4.6 PIEZOELECTRIC STIFFENING AND THE ELECTROMECHANICAL COUPLING CONSTANT

The Christoffel matrix for a piezoelectrically stiffened crystal is

$$\Gamma_{ij} = l_{iK}\left(c_{KL} + \frac{[e_{Kj}l_j][l_ie_{iL}]}{l_i\epsilon_{ij}^{S}l_j}\right)l_{Lj} \tag{4.59}$$

where l_{iK} and l_{Lj} are components of 3×6 and 6×3 matrices, respectively, and l_i and l_j are components of 1×3 and 3×1 matrices (column and row vectors). Whereas previously the Christoffel matrix depended only on

the direction of propagation and the stiffness matrix, we now must deal with the dielectric properties and piezoelectric properties of the material to determine the characteristics of acoustic propagation. We note that the piezoelectric corrections to the stiffness matrix depend not only on the **e** matrix, which in turn depends on the symmetry class, but also on the direction of propagation; a crystal may be strongly piezoelectric for a given direction while the effect is completely absent in a different direction. Piezoelectricity is always "coupled" to the direction of propagation or "cut" of the crystal.

From the form of (4.59), it is clear that the *stiffened* phase velocity is

$$v_a' = \sqrt{\frac{c'^{\mathbf{E}}}{\rho}} = \sqrt{\frac{c^{\mathbf{E}} + e^2/\epsilon^{\mathbf{S}}}{\rho}} \tag{4.60}$$

where all variables in (4.60) depend on $\hat{\mathbf{l}}$. To determine the piezoelectric correction quantitatively, we use the unstiffened phase velocity:

$$v_a = \sqrt{\frac{c^{\mathbf{E}}}{\rho}}$$

Note that this velocity is fictitious. The true velocity involves the stiffened constant c'. We use c simply as a mathematical convenience to calculate the effects of piezoelectricity on acoustic wave propagation. Rewriting (4.60), we obtain

$$v_a' = v_a(1 + K^2)^{1/2} \tag{4.61}$$

where

$$K^2 = \frac{e^2}{c^{\mathbf{E}}\epsilon^{\mathbf{S}}} \tag{4.62}$$

is called the *piezoelectric coupling constant*. We also define the *electromechanical coupling constant*:

$$k_t^2 = \frac{K^2}{1 + K^2} \tag{4.63}$$

where the subscript refers to the requirement that the electric field is applied across the thickness of the crystal. The electromechanical coupling constant is important when the piezoelectric crystal is used to convert electrical energy to mechanical energy (or *vice versa*). We will be using k_t^2 in Chapters 5 and 6 when we study electromechanical transducers; the rationale for two coupling constants will become clearer when we study acoustic resonators in Chapter 10. For most piezoelectric materials, $K^2 < 0.3$, so the difference between the two coupling constants is very small. For example, for the z-propagating longitudinal mode in ZnO:

$$K^2 = \frac{e_{33}^2}{c_{33}\epsilon_r} = .08$$

There is a simple interpretation for K^2 in terms of the energy carried by the electric and acoustic waves; recall the acoustic energy equation (not including attenuation) given by (1.28). In a piezoelectric medium, we add an electrical term so that (1.28) becomes

$$\frac{\partial}{\partial z}(-Tv) = j\omega(-c^E S^2 - \rho v^2 + \epsilon^S E^2) \tag{4.64}$$

Part of the mechanical energy is stored as the (longitudinal) electric field energy. The ratio of electric field energy to mechanical energy densities is

$$\frac{u_E}{u_M} = \frac{\epsilon^S E^2}{c^E S^2} \tag{4.65}$$

In the interior of the piezoelectric medium, the displacement vector vanishes (see (4.53)), so

$$E = -\frac{e^2}{\epsilon^S} S \tag{4.66}$$

Substituting (4.66) into (4.65) gives

$$\frac{u_E}{u_M} = \frac{e^2}{c^E \epsilon^S} = K^2$$

4.7 EXAMPLES OF PIEZOELECTRIC COUPLING

Example 4.1: Piezoelectricity in cubic crystals. We consider the piezoelectric correction to acoustic propagation in a principal plane (the xy plane) for cubic classes. The form of the piezoelectric matrix is given by (4.28) with all components equal. Performing the operations of (4.59), we obtain

$$\begin{aligned}\hat{\mathbf{l}}\mathbf{:e} &= (l_x\ l_y\ 0)\begin{bmatrix}0 & 0 & 0 & e & 0 & 0\\ 0 & 0 & 0 & 0 & e & 0\\ 0 & 0 & 0 & 0 & 0 & e\end{bmatrix}\\ &= (0\quad 0\quad 0\quad el_x\quad el_y\quad 0)\end{aligned} \tag{4.67}$$

Similarly;

$$\mathbf{e}:\hat{\mathbf{l}} = (\tilde{\hat{\mathbf{l}}}:\mathbf{e})$$

We then form

$$[\mathbf{e}:\hat{\mathbf{l}}]:[\mathbf{l}:\mathbf{e}] = \begin{bmatrix}0 & 0 & 0 & 0 & 0 & 0\\ 0 & 0 & 0 & 0 & 0 & 0\\ 0 & 0 & 0 & 0 & 0 & 0\\ 0 & 0 & 0 & e^2l_x^2 & e^2l_xl_y & 0\\ 0 & 0 & 0 & e^2l_xl_y & e^2l_y^2 & 0\\ 0 & 0 & 0 & 0 & 0 & 0\end{bmatrix} \tag{4.68}$$

The permittivity for a cubic matrix for cubic classes is a scalar ϵ_r (we develop the symmetry rules for permittivity in Chapter 7), so

$$l_i\epsilon_{ij}^{\mathbf{S}}l_j = \epsilon_r$$

The stiffened $\mathbf{c}$ matrix is

$$\mathbf{c}_s = \begin{bmatrix}c_{11} & c_{12} & c_{12} & 0 & 0 & 0\\ c_{12} & c_{11} & c_{12} & 0 & 0 & 0\\ c_{12} & c_{12} & c_{11} & 0 & 0 & 0\\ 0 & 0 & 0 & c'_{44} & c'_{45} & 0\\ 0 & 0 & 0 & c'_{45} & c'_{55} & 0\\ 0 & 0 & 0 & 0 & 0 & c_{66}\end{bmatrix} \tag{4.69}$$

where the primed components represent the stiffened c values:

$$c'_{44} = c_{44} + \frac{e^2 l_x^2}{\epsilon_r}, \quad c'_{45} = \frac{e^2 l_x l_y}{\epsilon_r}$$

$$c'_{55} = c_{44} + \frac{e^2 l_y^2}{\epsilon_r}$$

We next form the Christoffel matrix by using $\mathbf{c}_s$,

$$\Gamma = \begin{bmatrix} c_{11} l_x^2 & c_{12} l_x l_y & 0 \\ c_{12} l_x l_y & c_{11} l_y^2 & 0 \\ 0 & 0 & c_{44} + \dfrac{e^2 l_x l_y}{\epsilon_r} \end{bmatrix} \tag{4.70}$$

where e is the value of the three (equal) piezoelectric stress matrix components. We can draw four important conclusions immediately by inspecting (4.70):

1. Only the pure shear mode is piezoelectrically active in the principal planes.
2. The pure shear mode remains pure (it is polarized in the z direction for this example).
3. The velocity is no longer independent of direction because the stiffness constant is direction-dependent; thus, the slowness curve is no longer a circle, and the power flow angle no longer zero.
4. Along the principal axes, piezoelectricity vanishes; the maximum coupling is along $\langle 1, 1, 0 \rangle$.

To find the electrical potential, we use (4.45), where the velocity is given by

$$v_j = \begin{bmatrix} 0 \\ 0 \\ v_a \end{bmatrix}$$

and l_{Lj} is the 6×3 matrix given by (1.85). Carrying out the matrix multiplications, we arrive at

$$\phi = \frac{2 l_x l_y v_a e}{-j\omega\epsilon_r} \tag{4.71}$$

The electric field is

$$\mathbf{E} = -\nabla\phi = (jk)l_j(\phi) = \frac{2l_x l_y e}{\epsilon_r}(l_x\hat{\mathbf{i}} + l_y\hat{\mathbf{j}}) \tag{4.72}$$

The electric field is parallel to the propagation direction $\hat{\mathbf{l}}$, and the maximum potential (and field) occurs along $\langle 1, 1, 0\rangle$, as expected.

Example 4.2. We next consider the propagation of acoustic waves in two important crystals in the trigonal class: lithium niobate and crystal (α) quartz. For lithium niobate (class $3m$), the stiffness matrix is given by (4.56). To determine the propagation characteristic, we require the piezoelectric stress and permittivity matrices:

$$\mathbf{e} = \begin{bmatrix} 0 & 0 & 0 & 0 & e_{15} & -e_{22} \\ -e_{22} & e_{22} & 0 & e_{15} & 0 & 0 \\ e_{31} & e_{31} & e_{33} & 0 & 0 & 0 \end{bmatrix} \tag{4.73}$$

and

$$\boldsymbol{\epsilon} = \begin{bmatrix} \epsilon_{11} & 0 & 0 \\ 0 & \epsilon_{11} & 0 \\ 0 & 0 & \epsilon_{33} \end{bmatrix} \tag{4.74}$$

For x propagations:

$$\hat{\mathbf{l}} = \langle 1\ 0\ 0\rangle$$

Carrying out the operations from (4.46), we obtain the 1×6 (row) matrix:

$$\mathbf{l{:}e} = [0\ 0\ 0\ 0\ e_{15}\ -e_{22}]$$

The term $\mathbf{e{:}l}$ is simply the transpose of $\mathbf{l{:}e}$ and is a 6×1 (column) matrix:

$$\begin{bmatrix} 0 \\ 0 \\ 0 \\ 0 \\ e_{15} \\ -e_{22} \end{bmatrix}$$

The product of the two matrices $\mathbf{l{:}e}$ and $\mathbf{e{:}l}$ is the 6×6 matrix (note that the order of multiplication is important):

$$[\mathbf{l}:\mathbf{e}]:[\mathbf{e}:\mathbf{l}] = \begin{bmatrix} 0 & 0 & 0 & 0 & 0 & 0 \\ 0 & 0 & 0 & 0 & 0 & 0 \\ 0 & 0 & 0 & 0 & 0 & 0 \\ 0 & 0 & 0 & 0 & 0 & 0 \\ 0 & 0 & 0 & 0 & e_{15}^2 & -e_{15}e_{22} \\ 0 & 0 & 0 & 0 & -e_{15}e_{22} & e_{22}^2 \end{bmatrix} \tag{4.75}$$

Next, we determine the denominator of (4.46):

$$\boldsymbol{\epsilon}^{\mathbf{S}}:\mathbf{l} = \begin{bmatrix} e_{11} & 0 & 0 \\ 0 & \epsilon_{11} & 0 \\ 0 & 0 & \epsilon_{33} \end{bmatrix} \begin{bmatrix} 1 \\ 0 \\ 0 \end{bmatrix} = \begin{bmatrix} \epsilon_{11} \\ 0 \\ 0 \end{bmatrix} \tag{4.76}$$

and

$$\tilde{\mathbf{l}}:\boldsymbol{\epsilon}^{\mathbf{S}}:\mathbf{l} = [1\ 0\ 0]\begin{bmatrix} \epsilon_{11} \\ 0 \\ 0 \end{bmatrix} = \epsilon_{11} \tag{4.77}$$

As in (4.68), each term of (4.75) is divided by the scalar ϵ_{11} and added to the corresponding stiffness component to form the stiffened stiffness matrix:

$$\mathbf{c}_s = \begin{bmatrix} c_{11} & c_{12} & c_{13} & c_{14} & 0 & 0 \\ c_{12} & c_{11} & c_{13} & -c_{14} & 0 & 0 \\ c_{13} & c_{13} & c_{33} & 0 & 0 & 0 \\ c_{14} & -c_{14} & 0 & c_{44} & 0 & 0 \\ 0 & 0 & 0 & 0 & c'_{44} & c'_{14} \\ 0 & 0 & 0 & 0 & c'_{14} & c'_{66} \end{bmatrix} \tag{4.78}$$

where

$$c'_{44} = c_{44} + \frac{e_{15}^2}{\epsilon_{11}}, \quad c'_{14} = c_{14} - \frac{e_{15}e_{22}}{\epsilon_{11}}, \quad c'_{66} = c_{66} + \frac{e_{22}^2}{\epsilon_{11}}$$

We note that the stiffened **c** matrix is still symmetric; piezoelectricity cannot cause an unsymmetric stiffness matrix because the result would be an unsymmetric Christoffel matrix and unreal eigenvalues.

Now we use the corrected stiffness matrix to form the Christoffel matrix; carrying out the operations (2.51), we find

$$\Gamma = \begin{bmatrix} c_{11} & 0 & 0 \\ 0 & c'_{66} & c'_{14} \\ 0 & c'_{14} & c'_{44} \end{bmatrix} \tag{4.79}$$

where the primed components are piezoelectrically stiffened. Equation (4.79) indicates that the longitudinal mode (a pure mode because it is x-polarized) is not piezoelectrically active (c_{11} is unprimed); the phase velocity is simply

$$v_a = \sqrt{\frac{c_{11}}{\rho}}$$

The other two (pure shear modes, because they are polarized in the yz plane) are piezoelectrically active. We will solve the characteristic equation after we consider x propagation in α quartz.

Crystal (α) quartz is also trigonal, but its symmetry (class 32) is different from that of lithium niobate (class $3m$). The different symmetry elements result in a different form for the piezoelectric matrix (but not for the stiffness matrix). The form of **e** is

$$\mathbf{e} = \begin{bmatrix} e_{11} & -e_{11} & 0 & e_{14} & 0 & 0 \\ 0 & 0 & 0 & 0 & -e_{14} & -e_{11} \\ 0 & 0 & 0 & 0 & 0 & 0 \end{bmatrix} \tag{4.80}$$

Carrying out the operations to find the Christoffel matrix, we get

$$\Gamma = \begin{bmatrix} c'_{11} & 0 & 0 \\ 0 & c_{66} & c_{14} \\ 0 & c_{14} & c_{44} \end{bmatrix} \tag{4.81}$$

where

$$c'_{11} = c_{11} + \frac{e_{11}^2}{\epsilon_{11}} \tag{4.82}$$

In this case, the two shear modes (polarized in the yz plane) are piezoelectrically inactive (unprimed) while the longitudinal mode (x-polarized) is piezoelectrically active. Thus, applying an external electric field to an (x)-cut of lithium niobate (or lithium tantalate) will excite two shear modes but not a longitudinal mode, whereas an electric field applied to the same cut of quartz excites the longitudinal mode but not the two shear modes.

We now examine quantitatively the effect of piezoelectricity in these crystals. Consider the piezoactive longitudinal mode in ⟨x⟩ quartz. Using the formalism of (4.62), we see clearly that the piezoelectric coupling constant is

$$K_2 = \frac{e_{11}^2}{c_{11}^{\mathbf{E}} \epsilon_{11}} \tag{4.83}$$

If we substitute the relevant values for α quartz in (4.83), we get

$$c_{11} = 8.67 \times 10^{10}\ \mathrm{N/m^2}, \quad e_{11} = .17\ \mathrm{C/m}, \quad \epsilon_{11} = 4.5\epsilon_0$$

We find that

$$K^2 = 8.47 \times 10^{-3} \approx k^2$$

This is a typical value for the coupling constant of most of the useful piezoelectric cuts of quartz and is much less than some of the ferroelectric crystal we will consider. The utility of quartz is due to its relatively low acoustic attenuation and the availability of zero-temperature-dependent cuts; in addition, it is generally chemically inert, quite hard (making it relatively easy to polish), and available in optical quality at reasonable cost.

For lithium niobate, the characteristic equation for the piezoelectrically coupled shear modes has the form:

$$\begin{vmatrix} A - \lambda & B \\ B & C - \lambda \end{vmatrix} = 0$$

where

$$A = c'_{66} = c_{66} + \frac{e_{15}^2}{\epsilon_{11}}, \quad B = c'_{14} = c_{14} - \frac{e_{15}e_{22}}{\epsilon_{11}}$$

$$C = c_{44} + \frac{e_{22}^2}{\epsilon_{11}}$$

The solution is quite simple in terms of A, B, and C, but complex in terms of the stiffness constants because of the presence of the off-diagonal terms. We will develop computer-aided solutions to the problem, but for now we can get an approximate solution; the relevant constants are

$$c_{66} = 75 \times 10^9 \text{ N/m}^2$$

$$c_{44} = 60 \times 10^9 \text{ N/m}^2$$

$$c_{16} = 9 \times 10^9 \text{ N/m}^2 = c_{14}$$

$$e_{15} = 3.7 \text{ C/m}$$

$$e_{22} = 2.2 \text{ C/m}$$

$$\epsilon_{11} = 44_{\epsilon 0}$$

Now $c_{16} \ll c_{66}$ and $c_{16} \ll c_{44}$, so we assume that the off-diagonal terms are negligible (this assumption is grossly incorrect when we are solving for the eigenvectors); the coupling constants follow immediately from this approximation:

$$\text{for } c'_{66}: \quad K^2 = \frac{e_{22}^2}{c_{66}\epsilon_{11}} = .16 \quad \text{(slow shear mode)}$$

$$\text{for } c'_{44}: \quad K^2 = \frac{e_{15}^2}{c_{44}\epsilon_{11}} = .59 \quad \text{(fast shear mode)}$$

The values are .03 and .88, respectively. We note that they are extremely large compared with the coupling constants for crystal quartz. The fast shear (high coupling) mode in $\langle x \rangle$ lithium niobate possesses the strongest coupling constant of any single crystal material. The disadvantages are as follows: (1) The temperature stability of this cut is quite poor (lithium niobate contains no temperature-stable cuts). (2) The relatively high dielectric constant makes radio-frequency (RF) matching difficult. (3) The second mode is always excited and, even though its coupling is small, drains energy from the primary mode and may interfere in certain critical processes.

Example 4.3. As a final example, we consider $\langle z \rangle$ barium sodium niobate, which belongs to the orthorhombic class $2mm$. The form of the stiffness matrix is given in (2.114). The piezoelectric stress matrix has the form:

$$\mathbf{e} = \begin{bmatrix} 0 & 0 & 0 & 0 & e_{15} & 0 \\ 0 & 0 & 0 & e_{24} & 0 & 0 \\ e_{31} & e_{32} & e_{33} & 0 & 0 & 0 \end{bmatrix} \tag{4.84}$$

Carrying out the operations of (4.46), we obtain

$$\mathbf{l}:\mathbf{e} = [0\ 0\ 1]:\mathbf{e} = [e_{31} \quad e_{32} \quad e_{33} \quad 0 \quad 0 \quad 0]$$

and

$$\mathbf{e}:\mathbf{l} = \begin{bmatrix} e_{31} \\ e_{32} \\ e_{33} \\ 0 \\ 0 \\ 0 \end{bmatrix} = \tilde{(\mathbf{l}:\mathbf{e})}$$

From (4.46)

$$l_i \epsilon_{ij} l_j = \epsilon_{33}$$

The piezoelectrically stiffened matrix is

$$\mathbf{c}_s = \begin{bmatrix} c_{11} + \dfrac{e_{31}^2}{\epsilon_{33}} & c_{12} + \dfrac{e_{31}e_{32}}{\epsilon_{33}} & c_{13} + \dfrac{e_{31}e_{33}}{\epsilon_{33}} & 0 & 0 & 0 \\ c_{12} + \dfrac{e_{31}e_{32}}{\epsilon_{33}} & c_{22} + \dfrac{e_{32}^2}{\epsilon_{33}} & c_{23} + \dfrac{e_{32}e_{33}}{\epsilon_{33}} & 0 & 0 & 0 \\ c_{13} + \dfrac{e_{31}e_{33}}{\epsilon_{33}} & c_{23} + \dfrac{e_{32}e_{33}}{\epsilon_{33}} & c_{33} + \dfrac{e_{33}^2}{\epsilon_{33}} & 0 & 0 & 0 \\ 0 & 0 & 0 & c_{44} & 0 & 0 \\ 0 & 0 & 0 & 0 & c_{55} & 0 \\ 0 & 0 & 0 & 0 & 0 & c_{66} \end{bmatrix}$$

Using the l_{Kj} and l_{iK} matrices, we arrive at the Christoffel matrix for the important z-cut:

$$\mathbf{\Gamma} = \begin{bmatrix} c_{55} & 0 & 0 \\ 0 & c_{44} & 0 \\ 0 & 0 & c_{33} + \dfrac{e_{33}^2}{\epsilon_{33}} \end{bmatrix} \tag{4.85}$$

where, as usual,

$$k^2 \Gamma_{ij} v_j = \rho\omega^2 v_i$$

Even though every longitudinal term in the stiffness matrix was piezoelectrically stiffened, the Christoffel matrix has a simple form. Because there are always two shear modes (in this case unstiffened), they appear

with x and y polarizations (recall that the acoustic wave propagation is z), and the one longitudinal mode is positioned in the lower right (z-polarized) position. The shear velocities are simply,

$$v_a = \sqrt{\frac{c_{55}}{\rho}} \quad x\text{-polarized mode}$$

$$v_a = \sqrt{\frac{c_{44}}{\rho}} \quad y\text{-polarized mode}$$

A shear degeneracy does not exist for the z-propagating mode in the orthorhombic class because the "spring" constants are different for the x and y directions (compared with the tetragonal class in which $c_{44} = c_{55}$). From (4.85), it is obvious that the z-polarized longitudinal wave is piezoactive with coupling constant:

$$K^2 = \frac{e_{33}^2}{c_{33}\epsilon_{33}} \tag{4.86}$$

which has the same form as the z longitudinal cut in the hexagonal crystal ZnO. For barium sodium niobate, $e_{33} = 4.3$ C/m, $c_{33} = 135 \times 10^9$ N/m^2, and $\epsilon_{33} = 32\epsilon_0$ F/m. Substituting these values in (4.86) gives $K^2 = .48$ and $k_t^2 = .33$. This is the highest measured coupling constant for a longitudinal mode in a single-crystal material. In addition, the dielectric constant is somewhat lower than in other ferroelectrics. The electrical potential is given by (4.45). Carrying out the relevant operations, we obtain

$$\phi = \frac{v_a e_{33}}{j\omega\epsilon_{33}^S} \tag{4.87}$$

and

$$\mathbf{E} = -\nabla\phi = -\frac{e_{33}}{\epsilon_{33}}\hat{\mathbf{k}} \tag{4.88}$$

As in Example 4.1, the electric field is longitudinal to the acoustic wave propagation direction with a magnitude proportional to the acoustic wave.

There is an alternative technique, which uses (4.60), for determining the coupling constant for any crystal class and any direction of acoustic propagation:

1. Solve the Christoffel equation and determine the phase velocities *without* using the piezoelectric stress matrix (we again note that these are fictitious velocities).
2. Resolve the Christoffel equation a second time, using the stiffened stiffness matrix.
3. For each mode, form the ratio:

$$K^2 = \frac{(v_a - v_a')^2}{v_a^2} \sim \frac{2\Delta v_a}{v_a}$$

   where v_a and v_a' are the stiffened and unstiffened velocities and Δv_a is their difference.
4. Form the ratio:

$$k_i^2 = \frac{K^2}{1 + K^2}$$

This technique is especially well suited to computer-aided analysis as described in the next section.

4.8 COMPUTER-AIDED ANALYSIS OF PIEZOELECTRICALLY STIFFENED MODES

As we have seen, the calculation of piezostiffened velocities is quite cumbersome, even along the principal axes. The computer analysis discussed in Chapter 3 can easily be modified to include the effects of piezoelectricity. The strategy is to form the stiffened stiffness matrix **c** using the correction of (4.46) or (4.59). As we have previously remarked, the **c** components are no longer independent of the acoustic wave propagation direction because the correction terms depend on $\hat{\mathbf{l}}$, but the matrices l_{Lj}, l_{iL}, and the vector $\hat{\mathbf{l}}$ are related in a simple manner. The program module that calculates the stiffened **c** is shown in Figure 4.4. This module uses (4.59) to calculate the 6 × 6 correction matrix as a function of the permittivity and piezoelectric matrices and propagation direction vector $\hat{\mathbf{l}}$; it is placed after line 2620 in the program of Figure 3.1.

The additional input data required are the 3 × 6 permittivity matrix, denoted as EP33 (line 2710), and the 3 × 6 piezoelectric stress matrix, denoted by E36 (line 2800). These matrices are read into the program in the data block. The matrices LE16 and EL61 in lines 2800 and 2830 represent the terms $l_i e_{iL}$ and $e_{Kj} l_j$ in (4.59). Figure 4.5 shows the slowness

```
2650  ! THIS ROUTINE FINDS THE PIEZOELECTRIC STIFFENING CORRECTION
2680  MAT L31=TRN(L13)  ! TRANSPOSE OF L13
2710  MAT EL31 =EP33*L31
2740  LET DEN=EL31(1,1)*L13(1,1)+EL31(2,1)*L13(1,2)+EL31(3,1)*L13(1,3)
2770  LET DEN=DEN*.008854  !THIS IS THE DENOMINATOR OF THE CORRECTION
2800  MAT LE16= L13*E36
2830  MAT EL61= TRN(LE16)
2860  MAT CC66 = EL61*LE16  ! THIS IS THE NUMERATOR OF THE CORRECTION
2990  LET DEN=1/DEN
2920  MAT CC66= (DEN)*CC66  !THIS IS THE PIEZOELECTRIC CORRECTION MATRIX
2950  MAT CS66=C66+CC66 !THIS IS THE STIFFENED STIFFNESS MATRIX
```

Figure 4.4 Program listing for determination of piezoelectric stiffening; this module is placed after line 2620 in the program of Figure 3.1

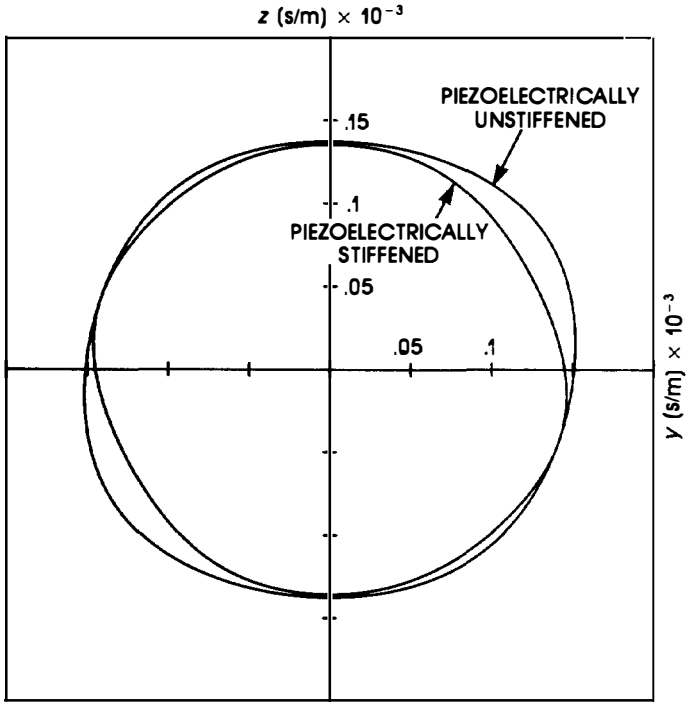

Figure 4.5 Piezoelectrically stiffened and unstiffened slowness curves for the quasilongitudinal mode in $LiNbO_3$ in the *yz* plane. Note that the difference between them is maximum at 30°. Only the stiffened curve is physically real.

curve of the longitudinal mode of lithium niobate in the *yz* plane. The difference between the stiffened and the unstiffened curves is a measure

of the piezoelectricity. Thus, there is a strong longitudinal response around 30°.

Similarly, by plotting the stiffened and unstiffened shear slowness curves it is not difficult to show that there is a strong shear response near 160°. Figure 4.6 shows the stiffened and unstiffened slowness curves of the pure shear mode in InSb (a strongly piezoelectric cubic crystal). Note that the stiffening is a maximum at 45° to the principal axes, which is consistent with (4.70). Figure 4.7 shows the stiffened and unstiffened slowness curves for orthorhombic sodium barium niobate ($Ba_2NaNb_5O_{15}$). The high coupling longitudinal z-cut is clearly shown. Of special interest is the curvature of this mode near the z-axis, which exhibits a focusing effect; this is the only known example of a longitudinal mode in which this occurs [7].

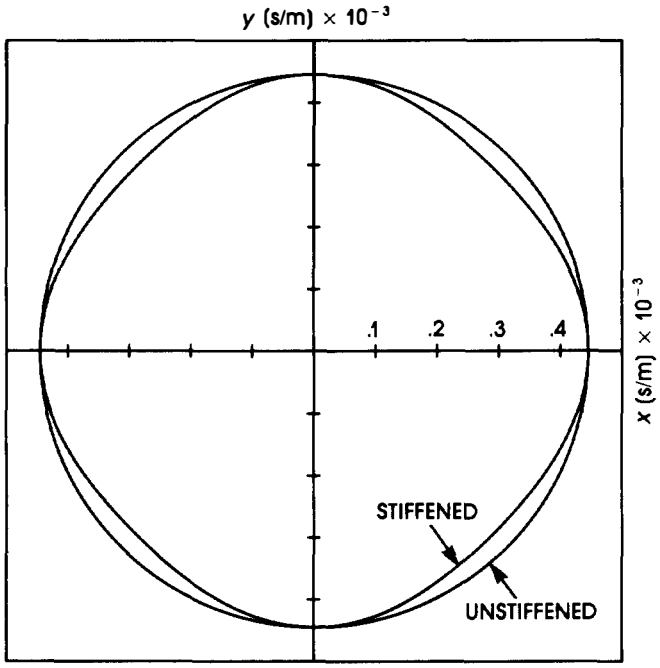

Figure 4.6 Piezoelectrically stiffened and unstiffened slowness curves for the pure shear mode InSb (which possesses a large piezocoupling component). The difference is a maximum at 45°.

To calculate the electromechanical coupling constant, we follow the formula outlined in the previous section. Using the stiffened **c** matrix, we solve the Christoffel equation by standard techniques, yielding the three

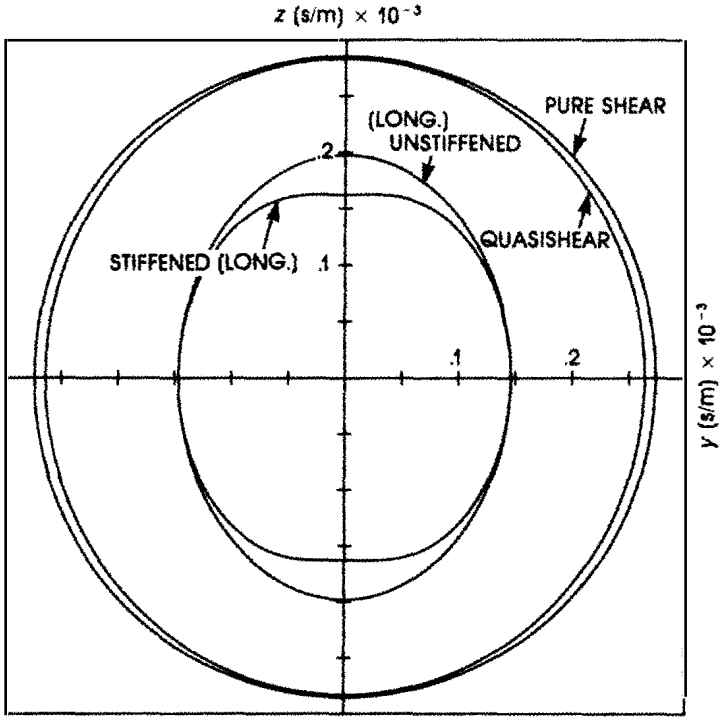

Figure 4.7 Stiffened and unstiffened slowness curves of barium sodium niobate. The stiffened longitudinal curve is compatible with anisotropic acoustic focusing along the z-axis.

phase velocities. For the same acoustic propagation direction, the *unstiffened* $\mathbf{c}$ is used to resolve for the phase velocities. For each mode, K^2 is determined by (4.61).

Figure 4.8 shows the results of this procedure for $LiNbO_3$ in the xy plane. The high coupling of the fast shear mode for the x-cut and the fact that it is a pure mode make this the most useful orientation. There is no direction in which only one mode is piezoactive in this plane. Pure modes exist only along the x- and y-axes. Figure 4.9 shows the coupling in the yz plane. Here the pure shear mode is piezoactive for all orientations. The most useful one, however, is at 163°, because at this cut it is the only piezoactive mode. For this reason, this mode is quite popular even though its coupling is somewhat less than that of the x-cut. A second useful mode in this plane is the 36° y-cut longitudinal mode. The maximum longitudinal

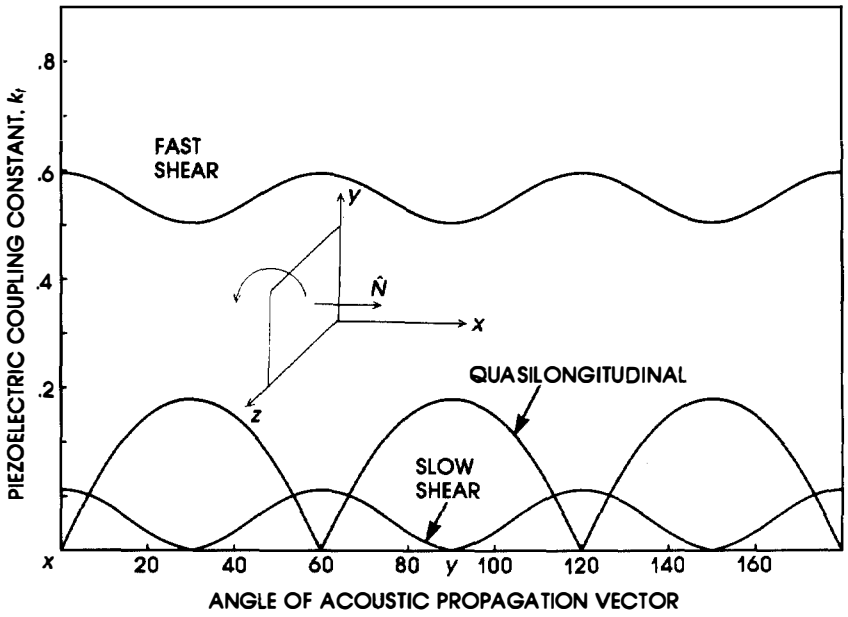

Figure 4.8 Piezocoupling of $LiNbO_3$ in the xy plane. Note the symmetry of the curves, the extraordinarily high coupling for ⟨x⟩ shear, and the fact that there are no cuts with only one piezoactive mode.

coupling occurs at 30°, but at 36° the shear coupling vanishes. The only disadvantage of this mode is that it is not a pure mode (the deviation angle is approximately 4°). Finally, Figure 4.10 shows the piezocoupling in the yz plane of sodium barium niobate. As expected, the useful cut is the z longitudinal mode.

Because the piezoelectric stiffening alters the components of the stiffness matrix, this stiffening also affects not only the shape of the slowness curve (and thus the power flow angle) but also the direction of the polarizations. Figure 4.11 shows the deviation from pure mode direction for the piezoelectrically stiffened longitudinal mode in the yz plane of lithium niobate and for the unstiffened (fictitious) case. Note that for z orientation the longitudinal mode is pure.

Table 4.2 lists common high frequency transducer materials and their properties.

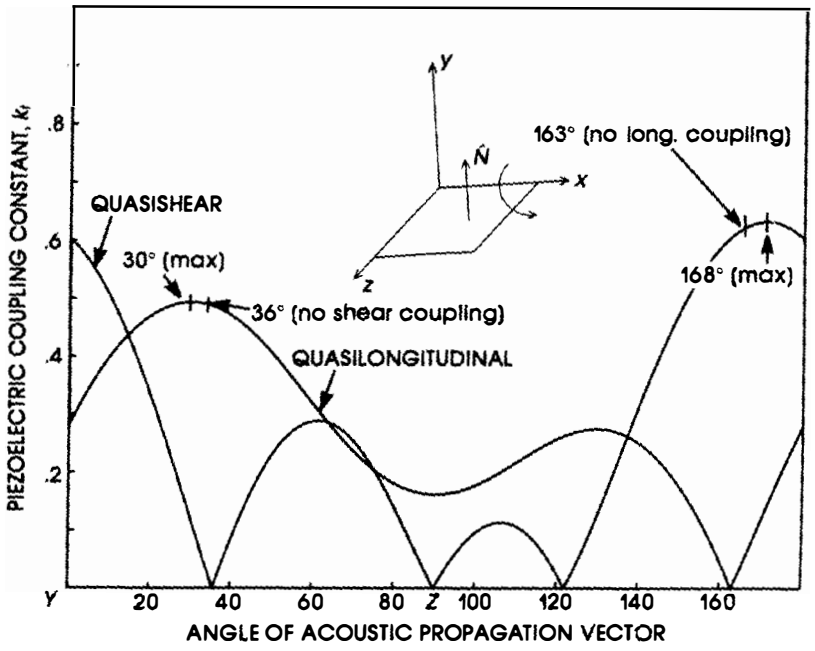

Figure 4.9 Piezocoupling of $LiNbO_3$ in the yz plane. There are two important cuts: the 36° $\langle y \rangle$ (longitudinal) and 163° $\langle y \rangle$ shear. In both cases, only one mode is excited, each of which is a quasimode.

Table 4.2

Material and Cut	*Impedance*	k_t^2	*Advantages*	*Disadvantages*
36° $\langle y \rangle$ $LiNbO_3$ (longitudinal)	3.4×10^7	.25	High coupling high velocity	Not pure mode high permittivity
$\langle x \rangle$ $LiNbO_3$ (shear)	2.2×10^7	.46	High coupling	Two excited modes high permittivity
163° $\langle y \rangle$ $LiNbO_3$ (shear)	2×10^7	.38	High coupling	High permittivity
$\langle z \rangle$ ZnO (longitudinal)	3.5×10^7	.08	Low permittivity pure mode	Low coupling difficult to deposit
$\langle x \rangle$ SiO_2 (longitudinal)	1.5×10^7	8.5×10^{-3}	Low permittivity pure mode	Low coupling
$Ba_2NaNb_5O_{15}$ (longitudinal)	3.2×10^7	.33	High coupling pure mode	Material availability

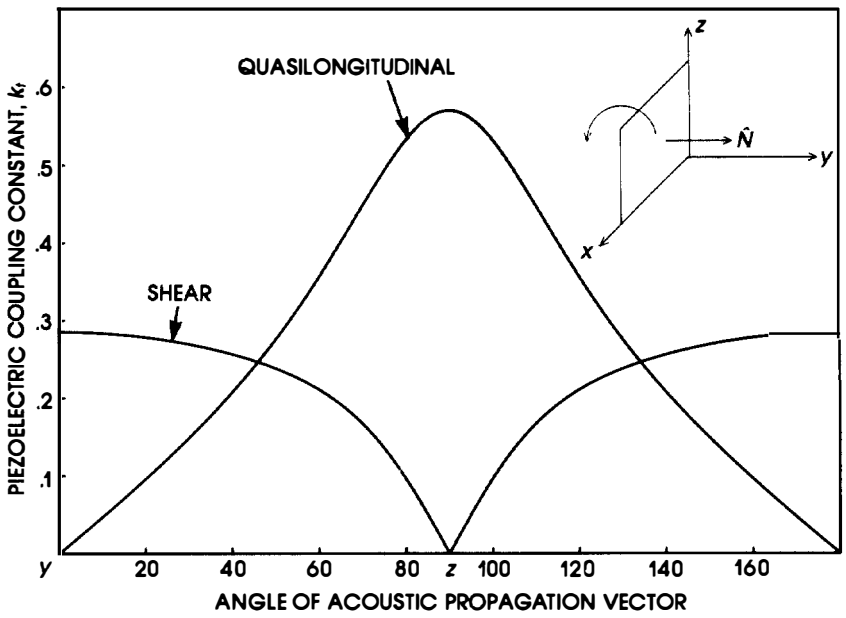

Figure 4.10 Piezocoupling of barium sodium niobate in the yz plane. The $\langle z \rangle$ longitudinal mode has very high coupling and is a pure mode.

4.9 PIEZOELECTRIC COUPLING IN DOUBLY ROTATED ORIENTATIONS

The curves in Figures 4.8 to 4.10 show the coupling constant in the principal planes. Using the formalism of the previous section, it is not difficult to determine the coupling for an arbitrary direction of acoustic wave propagation. A general direction in Cartesian space can be thought of as a doubly rotated orientation, or "cut," because it can be derived by two rotations about the principal axes. Figure 4.12 shows the piezoelectric coupling constant k_t for the longitudinal mode in lithium niobate for a series of doubly rotated cuts. These curves are derived by the following procedure:

1. Rotate the crystal a fixed angle ϕ about the z-axis to form a new coordinate system with axes x', y', z. The, $\phi = 0$ corresponds to the y-z plane, while $\phi = 90°$ corresponds to the x-z plane.

2. Rotating about the x' axis; k_t is determined, as usual, by forming the difference between stiffened and unstiffened velocities.

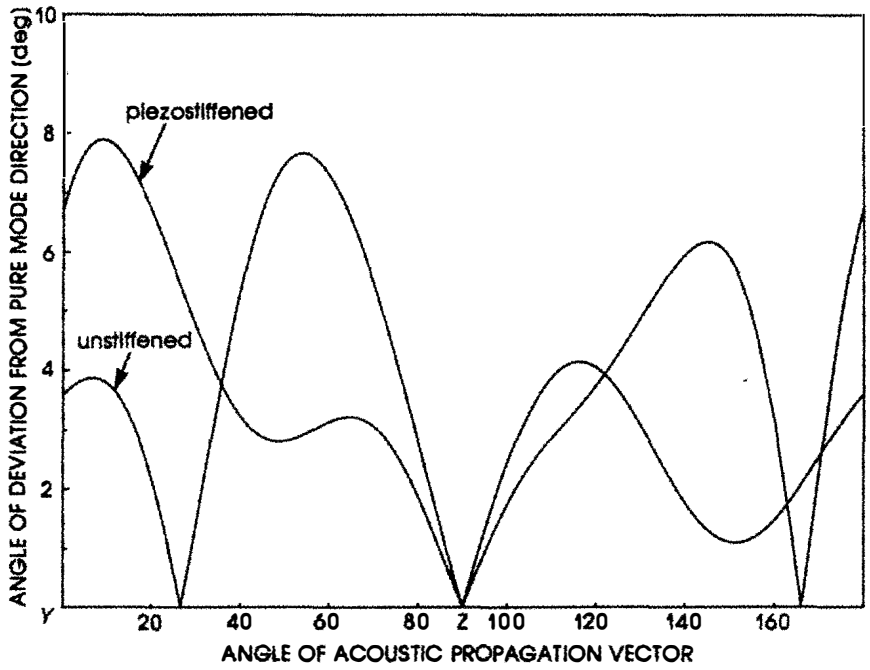

Figure 4.11 Deviation angle from the pure mode direction of $LiNbO_3$ in the yz plane for stiffened and unstiffened modes. Note the large effect of stiffening on the deviation angles.

The curves reveal that the doubly rotated cut $\phi = 60°$, $\theta = 150°$, possesses a high coupling constant ($k_t = .49$). This orientation has a somewhat smaller deviation angle than the singly rotated cut. The doubly rotated cut is not used in practical transducers because of the added complexity in performing the required two rotations. For crystal quartz, however, there are doubly rotated cuts with significant performance advantages, which more than compensate for the additional fabrication difficulty.

PROBLEMS

4.1 Show that the velocities of the longitudinal and shear modes in the xy plane of hexagonal calsses are given by

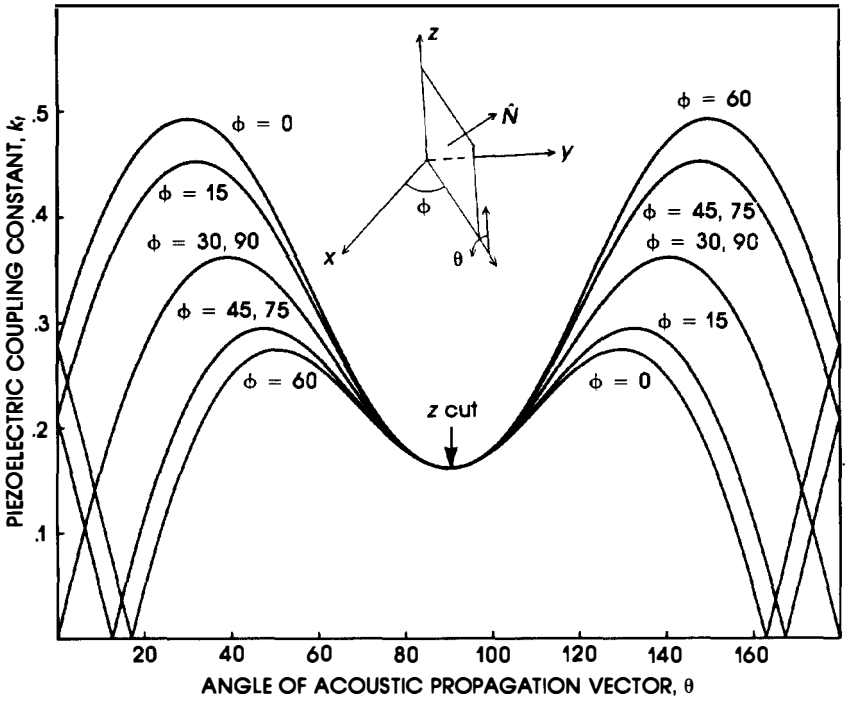

Figure 4.12 Longitudinal coupling constant of doubly rotated cuts of lithium niobate.

$$\text{longitude: } v_a = \sqrt{\frac{c_{11}}{\rho}}$$

$$\text{shear 1: } v_a = \sqrt{\frac{c_{66}}{\rho}} \qquad \sqrt{\frac{c_{11}}{}}$$

$$\text{shear 2: } v_a = \sqrt{\frac{c_{44}}{\rho}}$$

4.2 Derive the form of the Christoffel matrix for the trigonal class $3m$, using the stiffness matrix in (4.56).

4.3 Use Neumann's principle to derive the form of the **e** for the class 4*mm* (tetragonal).

4.4 Complete the derivation of (4.55).

4.5 Find the coupling constant of ⟨*x*⟩ and ⟨*y*⟩ ZnO.

4.6 For propagation along the *y*-axis of lithium niobate there is one pure (shear) mode and two quasimodes. Determine the polarization and the deviation angles for the two quasimodes.

4.7 Repeat Problem 4.6 for crystal quartz.

4.8 Only the shear mode is piezoelectrically active for the cubic symmetry in the principal planes, and the longitudinal mode can be excited in an arbitrary plane. Determine k_t for InSb for the ⟨1, 1, 1⟩ direction.

REFERENCES

1. B. Auld, *Acoustic Fields and Waves in Solids,* John Wiley and Sons, New York, 1973, Chapter 9.
2. J. Nye, *Physical Properties of Crystals,* Oxford University Press, London, 1957, Chapter 7.
3. Z. Turski, *et al.*, "Properties of an ⟨*x*⟩-cut Single Crystal Lithium Niobate Transducer," *IEEE Trans. Sonics and Ultrasonics,* **SU-22**(6) 402 (1975).
4. V. Bottom, *Introduction to Quartz Crystal Unit Design,* Van Nostrand, New York, 1982, Chapter 4.
5. W. Bond, *et al.*, " 'Elastic' Poynting Vector in a Piezoelectric Medium," *IEEE Trans. Sonics and Ultrasonics,* **SU-17** (4)246 (1970).
6. A. Warner, *et al.*, "Determination of Elastic and Piezoelectric Constants for Crystals . . ." *J. Acoust. Soc. Am.,* **42,** 1223 (1967).
7. A. Every and A. McCurdy, "Phono Focusing in Piezoelectric Crystals," *Phys. Rev. B,* **36** (3), 1432 (1987).